BJP BRITISH JOURNAL OF PHARMACOLOGY

BPS BRITISH PHARMACOLOGICAL SOCIETY

British Journal of Pharmacology (2009), 158, 1356–1365

0007-1188/09
www.brjpharmacol.org

RESEARCH PAPER

Phosphorylation alters the pharmacology of Ca^{2+}-activated Cl^- channels in rabbit pulmonary arterial smooth muscle cells

M Wiwchar[1], R Ayon[1], IA Greenwood[2] and N Leblanc[1]

[1]*Department of Pharmacology, Center of Biomedical Research Excellence (COBRE), University of Nevada School of Medicine, Reno, NV, USA, and* [2]*Division of Basic Medical Sciences, St George's, University of London, London, UK*

Background and purpose: Ca^{2+}-activated Cl^- currents ($I_{Cl(Ca)}$) in arterial smooth muscle cells are inhibited by phosphorylation. The Ca^{2+}-activated Cl^- channel (Cl_{Ca}) blocker niflumic acid (NFA) produces a paradoxical dual effect on $I_{Cl(Ca)}$, causing stimulation or inhibition at potentials below or above 0 mV respectively. We tested whether the effects of NFA on $I_{Cl(Ca)}$ were modulated by phosphorylation.
Experimental approach: $I_{Cl(Ca)}$ was elicited with 500 nM free internal Ca^{2+} in rabbit pulmonary artery myocytes. The state of global phosphorylation was altered by cell dialysis with either 5 mM ATP or 0 mM ATP with or without an inhibitor of calmodulin-dependent protein kinase type II, KN-93 (10 μM).
Key results: Dephosphorylation enhanced the ability of 100 μM NFA to inhibit $I_{Cl(Ca)}$. This effect was attributed to a large negative shift in the voltage-dependence of block, which was converted to stimulation at potentials <–50 mV, ~70 mV more negative than cells dialysed with 5 mM ATP. NFA dose-dependently blocked $I_{Cl(Ca)}$ in the range of 0.1–250 μM in cells dialysed with 0 mM ATP and KN-93, which contrasted with the stimulation induced by 0.1 μM, which converted to block at concentrations >1 μM when cells were dialysed with 5 mM ATP.
Conclusions and implications: Our data indicate that the presumed state of phosphorylation of the pore-forming or regulatory subunit of Cl_{Ca} channels influenced the interaction of NFA in a manner that obstructs interaction of the drug with an inhibitory binding site.
British Journal of Pharmacology (2009) **158,** 1356–1365; doi:10.1111/j.1476-5381.2009.00405.x; published online 28 September 2009

Keywords: Calcium-activated chloride channels; vascular smooth muscle; niflumic acid; phosphorylation; state-dependent block

Abbreviations: AMP-PNP, adenosine 5′-(β,γ-imido)-triphosphate; BAPTA, 1,2-bis(o-aminophenoxy)ethane-N,N,N′,N′-tetraacetic acid; BK_{Ca}, large conductance calcium-activated potassium channel; CaM, calmodulin; CaMKII, calmodulin-dependent protein kinase type II; Cl_{Ca}, calcium-activated chloride channel; CsA, cyclosporine A; HP, holding potential; I_{CaL}, L-type calcium current; $I_{Cl(Ca)}$, calcium-activated chloride current; I_{sK}, slow delayed rectifier potassium current; I-V, current–voltage relationship; NFA, niflumic acid; PA, pulmonary artery; PSS, physiological salt solution; SR, sarcoplasmic reticulum; STICs, spontaneous transient inward currents; $V_{0.5}$, half-maximal voltage; VSMC, vascular smooth muscle cell

Introduction

The membrane depolarization associated with the opening of Ca^{2+}-activated Cl^- channels (Cl_{Ca}) is thought to be an important contributor to the development of vascular smooth muscle tone induced by constricting hormones and neurotransmitters (Large and Wang, 1996; Leblanc *et al.*, 2005). Among several classes of agents, the non-steroidal anti-inflammatory drug, niflumic acid (NFA) has been extensively used as a 'relatively' selective blocker of Cl_{Ca} channels in vascular smooth muscle cells (VSMCs) (Large and Wang, 1996). At concentrations in the range of ~1–50 μM, NFA blocks Ca^{2+}-activated Cl^- currents ($I_{Cl(Ca)}$) evoked by L-type Ca^{2+} current (Yuan, 1997), reverse-mode Na^+/Ca^{2+} exchange (Leblanc and Leung, 1995), constricting agonists or caffeine (Hogg *et al.*, 1994), spontaneous transient inward Cl^- currents (STICs) triggered by spontaneous release of Ca^{2+} from the

Correspondence: Normand Leblanc, Department of Pharmacology/MS 318, Center of Biomedical Research Excellence (COBRE), University of Nevada School of Medicine, 1664 North Virginia, Reno, NV 89557-0270, USA. E-mail: NLeblanc@Medicine.Nevada.edu
Received 25 February 2009; revised 26 April 2009; 2 June 2009; accepted 5 June 2009

sarcoplasmic reticulum (SR) (Hogg *et al.*, 1994; Janssen and Sims, 1994; Greenwood and Large, 1995; ZhuGe *et al.*, 1998), or flash photolysis of caged Ca^{2+} (Clapp *et al.*, 1996). Within the same concentration range, NFA has no effect on the magnitude of Ca^{2+} current (Pacaud *et al.*, 1989; Lamb *et al.*, 1994; Yuan, 1997), swelling-activated Cl^- current (Greenwood and Large, 1998), KCl-induced contractions (Criddle *et al.*, 1996; 1997; Yuan, 1997; Lamb and Barna, 1998; Remillard *et al.*, 2000), or SR Ca^{2+} release evoked by caffeine or norepinephrine (Hogg *et al.*, 1994).

The effects of NFA on VSMC Cl_{Ca} channels are complex, with a wide range of IC_{50} values reported for blockade of these channels. A close examination of the studies that have investigated the effects of NFA on $I_{Cl(Ca)}$ suggests that its potency appears to be linked to the method used to evoke the current. Indeed, the IC_{50} for inhibiting STICs was <4 μM (Hogg *et al.*, 1994) whereas the affinity of NFA for blocking $I_{Cl(Ca)}$ evoked by an agonist or caffeine was at least twofold lower (Hogg *et al.*, 1994). Although dose–response relationships were not obtained, NFA appeared less efficacious at inhibiting arterial $I_{Cl(Ca)}$ elicited by inward Ca^{2+} current than STICs with 10 μM NFA producing ~50–80% of the deactivating Cl^- tail current recorded after return to the holding potential (HP) (Lamb *et al.*, 1994; Yuan, 1997). A further reduction in potency was evident during NFA-induced block of $I_{Cl(Ca)}$ evoked by elevated sustained intracellular Ca^{2+} concentration (500 nM) in coronary myocytes with an IC_{50} at +50 mV of 159 μM (Ledoux *et al.*, 2005). One possible explanation of these observations may relate to the ability of higher $[Ca^{2+}]_i$, either induced cyclically or maintained, to promote downregulation of $I_{Cl(Ca)}$ by phosphorylation via calmodulin-dependent protein kinase type II (CaMKII) (Wang and Kotlikoff, 1997; Greenwood *et al.*, 2001; 2004; Ledoux *et al.*, 2003; Angermann *et al.*, 2006).

The present study was undertaken to test the hypothesis that the presumed state of phosphorylation of Cl_{Ca} channel influences their pharmacology.To this end, we tested the effects of NFA on $I_{Cl(Ca)}$ evoked by 500 nM internal Ca^{2+} in rabbit pulmonary artery myocytes dialysed with either 5 mM ATP to induce global phosphorylation, or in the absence of ATP with or without the CaMKII inhibitor KN-93, to promote dephosphorylation of the channel or a regulatory protein (Angermann *et al.*, 2006). At positive potentials, the block displayed steep voltage dependence that was markedly attenuated in conditions favouring global dephosphorylation. On the other hand, Cl_{Ca} channels suppressed by conditions promoting global phosphorylation exhibited enhanced stimulation by NFA at negative potentials. These results demonstrate that the presumed state phosphorylation of the pore-forming or regulatory subunit of Cl_{Ca} channels has a profound influence on the interaction of NFA with these channels, which may explain the wide range of sensitivities of these channels to NFA reported in many earlier studies.

Methods

Isolation of rabbit pulmonary artery myocytes

All animal care and experimental procedures were approved by the University of Nevada Institutional Animal Care and Use Committee. The animals were allowed free access to food and water and kept on a 12–12 h light/dark cycle. Smooth muscle cells were isolated as described earlier (Greenwood *et al.*, 2004; Angermann *et al.*, 2006). In brief, cells were prepared from the main and secondary pulmonary arterial branches dissected from New Zealand white rabbits (2–3 kg) killed by anaesthetic overdose. After dissection and removal of connective tissue, the pulmonary arteries were cut into small strips and incubated overnight (~16 h) at 4°C in a low Ca^{2+} physiological salt solution (PSS; see composition below) containing either 10 or 50 μM $CaCl_2$ and ~1·mg·mL^{-1} papain, 0.15·mg·mL^{-1} dithiothreitol and 1·mg·mL^{-1} bovine serum albumin. The next morning, the tissue strips were rinsed three times in low Ca^{2+} PSS and incubated in the same solution for 5 min at 37°C. Cells were released by gentle agitation with a wide bore Pasteur pipette, and then stored at 4°C until used (within 10 h following dispersion).

Whole-cell patch clamp electrophysiology

Ca^{2+}-activated Cl^- currents were elicited using the conventional whole-cell configuration of the patch clamp technique with a pipette solution containing either 0 mM ATP with KN-93 (a specific inhibitor of CaMKII) or 5 mM ATP. The pipette solution also contained 10 mM BAPTA as the Ca^{2+} buffer and free $[Ca^{2+}]$ was set to 500 nM by the addition of 7.08 mM $CaCl_2$. The free $[Ca^{2+}]$ was estimated by the calcium chelator program WinMaxC (v. 2.50; http://www.stanford.edu/~cpatton/downloads.htm). Using a Ca^{2+}-sensitive electrode and calibrated solutions, the total amounts of $CaCl_2$ and $MgCl_2$ calculated by the software were previously shown to yield accurate free Ca^{2+} concentrations with both EGTA and BAPTA as Ca^{2+} buffers (Ledoux *et al.*, 2003; Greenwood *et al.*, 2004; Angermann *et al.*, 2006). Contamination of $I_{Cl(Ca)}$ from other types of current was minimized by the use of CsCl and tetraethylammonium chloride (TEA) in the pipette solution, and TEA in the external solution. Data for each group were collected in cells from at least two animals but generally more.

Experimental protocols

$I_{Cl(Ca)}$ was evoked immediately upon rupture of the cell membrane and the voltage-dependent properties were monitored every 5 or 10 s by stepping from a HP of –50 mV to +90 mV for 1 s, followed by repolarization to –80 mV for 1 s. Current–voltage (I–V) relationships were constructed by stepping in 10 mV increments from HP to test potentials between –100 mV and +140 mV for 1 s after 10 min dialysis. For I–V relationships, $I_{Cl(Ca)}$ was expressed as current density (pA/pF) by dividing the amplitude of the current measured at the end of the voltage clamp step by the cell capacitance. For all figure panels showing a time course of $I_{Cl(Ca)}$ changes, the late current measured at +90 mV was normalized to the amplitude of first current elicited at time = 0 (~30 s after breaking the seal and measuring cell capacitance). After measuring cell capacitance, the constant step protocol described above was started to monitor the changes of $I_{Cl(Ca)}$ over the course of 10 min after which a control I–V relationship was obtained. While monitoring $I_{Cl(Ca)}$ elicited by a similar constant step protocol described above, the external solution was switched to one

containing NFA at a concentration of 0.1, 1, 10, 100 or 500 μM. During these experiments, cells were stepped from the HP to +80 mV before being repolarized to –80 mV. After a steady-state effect was noticed, another I–V relationship was obtained in the presence of NFA. If the seal was still stable, washout was subsequently initiated and an I–V curve generated after washout. Only one concentration of NFA was tested per cell.

Solutions

Single pulmonary artery smooth muscle cells were isolated by incubating pulmonary artery tissue strips in the following low Ca^{2+} (10 or 50 μM) PSS (in mM): NaCl (120), KCl (4.2), $NaHCO_3$ (25; pH 7.4 after equilibration with 95% O_2 5% CO_2 gas), KH_2PO_4 (1.2), $MgCl_2$ (1.2), glucose (11), taurine (25), adenosine (0.01) and $CaCl_2$ (0.01 or 0.05). The K^+-free bathing solution used in all patch clamp experiments had the following composition (in mM): NaCl (126), HEPES-NaOH (10, pH 7.35), TEA (8.4), glucose (20), $MgCl_2$ (1.2) and $CaCl_2$ (1.8). The pipette solution had the following composition (in mM): TEA (20), CsCl (106), HEPES-CsOH (10, pH 7.2), BAPTA (10), ATP.Mg (0 or 5), GTP.diNa (0.2) and KN-93 (0 or 0.01). To this solution, the following total amounts of $CaCl_2$ and $MgCl_2$ were added to set free [Mg^{2+}] at 0.5 mM and free [Ca^{2+}] at various desired levels: 5 mM ATP and 500 nM Ca^{2+} (in mM): $CaCl_2$ (7.08), $MgCl_2$ (3.0); no ATP and 500 nM Ca^{2+}: $CaCl_2$ (7.08), $MgCl_2$ (0.545).

Statistical analysis

All data were pooled from *n* cells taken from at least two different animals with error bars representing the SEM. All data were first pooled in Excel and means exported to Origin 7.5 software (OriginLab, Northampton, MA, USA) for plotting and curve fitting. All graphs and current traces were exported to CorelDraw 12 (Ottawa, ON, Canada) for final processing of the figures. *Origin* 7.5 software (OriginLab, Northampton, MA, USA) was also used to determine the statistical significance between two groups using a paired or unpaired Student's *t*-test, or one-way ANOVA test followed by Bonferroni *post hoc* multiple range tests in multiple group comparisons. $P < 0.05$ was considered to be statistically significant.

Materials

All enzymes, analytical grade reagents and NFA were purchased from Sigma-Aldrich (St Louis, MO, USA). NFA was initially prepared as 1, 10 or 100 mM stock in dimethyl sulphoxide (DMSO) and an appropriate aliquot was added to the external solution to reach the final desired concentration. The maximal concentration of DMSO never exceeded 0.1%, a concentration that had no effect on $I_{Cl(Ca)}$.

Results

Effect of global phosphorylation status on Ca^{2+}-activated Cl^- current

In all experiments we systematically dialysed the cells for 10 min with 5 mM ATP, or 0 mM ATP with or without 10 μM KN-93, a specific inhibitor of CaMKII. KN-93 was added to facilitate a presumed state of dephosphorylation of the channel or regulatory subunit by endogenous phosphatases. As previously shown by our group (Greenwood *et al.*, 2001; 2004; Angermann *et al.*, 2006), these conditions allowed us to first establish conditions favouring completely different states of cellular phosphorylation before examining the effects of NFA on Ca^{2+}-activated Cl^- current ($I_{Cl(Ca)}$) evoked by 500 nM free intracellular Ca^{2+} concentration. Figure 1A-*a* shows current traces recorded at different times after seal rupture from two sample experiments under the conditions described above. $I_{Cl(Ca)}$ was evoked by 1 s steps to +90 mV from an HP of –50 mV which was followed by a 1 s repolarizing step to –80 mV before returning to the HP. As previously shown by our group (Greenwood *et al.*, 2001; 2004; Angermann *et al.*, 2006), step depolarization to +90 mV induced an initial instantaneous membrane current after the capacitative current that was followed by a slow time-dependent current component, both arising from basal and voltage-dependent gating properties of Ca^{2+}-activated Cl^-channels. A slow tail current was apparent upon repolarization to –80 mV and is consistent with channel closure caused by voltage-dependent deactivation. Immediately after seal rupture (0 min), $I_{Cl(Ca)}$ evoked in both conditions displayed similar amplitude and kinetics. $I_{Cl(Ca)}$ exhibited marked rundown during the first 2 min and remained suppressed throughout the initial 10 min of cell dialysis with 5 mM ATP. Removal of ATP and inclusion of KN-93 to suppress CaMKII activity in the pipette solution also resulted in $I_{Cl(Ca)}$ rundown but the magnitude of this process was clearly attenuated after 2 min. This initial rundown is most likely to reflect a partial state of phosphorylation of an unknown regulatory or pore-forming subunit because of consumption of endogenous levels of ATP before depletion ensues. With continued dialysis, $I_{Cl(Ca)}$ progressively recovered and eventually exceeded (see traces at 10 min) the amplitude of the initial current recorded at the onset of dialysis. The graph in Figure 1A-*b* shows mean data obtained from 32 or 42 cells in each group. For each data set, the amplitude of $I_{Cl(Ca)}$ recorded at the end of the step to +90 mV was normalized to that of the initial current recorded at time = 0. Consistent with the experiment described in Figure 1A-*a*, $I_{Cl(Ca)}$ exhibited marked rundown after breaking the seal with 5 mM ATP reaching ~15% of the initial level in less than 2 min, a level that remained very stable throughout the rest of the experiment. As in Figure 1A, removing ATP and the addition of KN-93 from the pipette attenuated the rundown and resulted in a complete recovery that continued to develop beyond the initial level (~30% above the initial level). The global state of phosphorylation also affected deactivation kinetics, where removal of ATP from the pipette solution caused a slowing of the time constant from 70.5 ± 3.4 ms ($n = 42$) to 101.9 ± 6.1 ms ($n = 32$; $P < 0.001$), with 5 mM ATP and no ATP and 10 μM KN-93 respectively. An opposite trend was observed for the activation kinetics although the differences were just at the limit of significance; τ for activation was 322.9 ± 11.1 ms for 5 mM ATP ($n = 42$) and 300.5 ± 14.1 ms for 0 mM ATP with KN-93 ($n = 32$; $P = 0.0576$). The effects of different ATP levels on $I_{Cl(Ca)}$ are very similar to those reported by Angermann *et al.* (2006) who proposed that phosphorylation causes a state-dependent block of the channels. Another

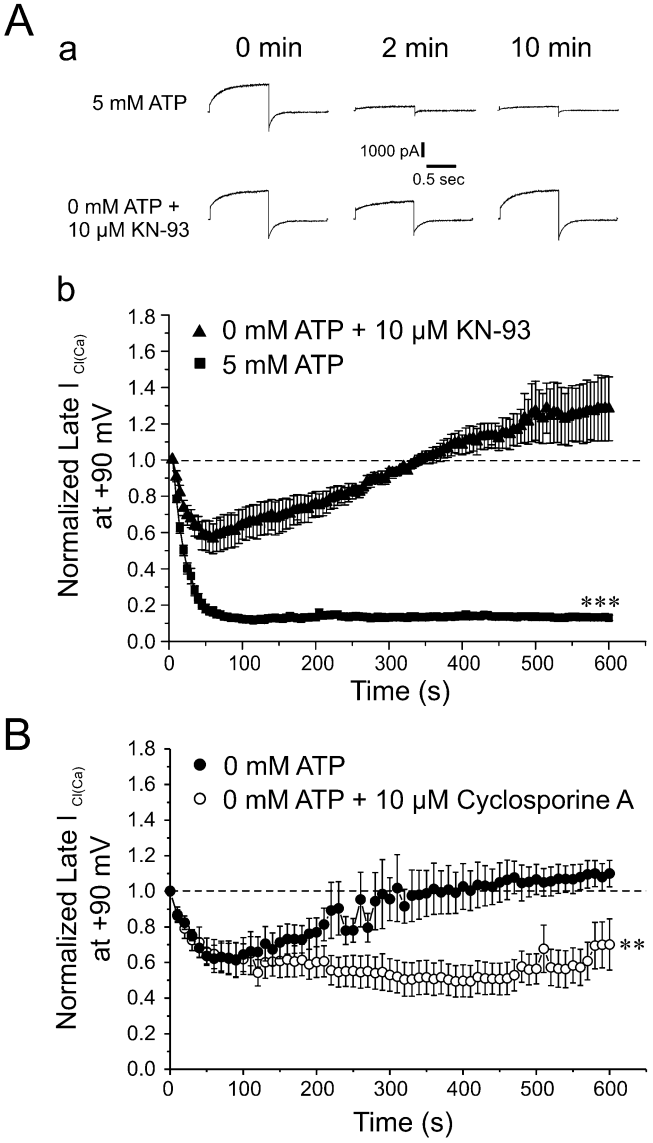

Figure 1 Attenuation of rundown of Ca^{2+}-activated Cl^- currents in rabbit pulmonary artery myocytes by minimizing phosphorylation. (A-*a*) Representative current traces demonstrate the time-dependent changes of Ca^{2+}-activated Cl^- current recorded from pulmonary arterial smooth muscle cells dialysed with either 5 mM ATP or 0 mM ATP + 10 μM KN-93. Currents depicted were recorded immediately following breaking the seal (0 min), and after 2 and 10 min of cell dialysis. The currents were elicited by repetitive 1 s step depolarizations (every 5 s) to +90 mV from a holding potential (HP) of −50 mV. Each depolarizing pulse was followed by a repolarizing step to −80 mV to enhance the magnitude of the tail current. (A-*b*) This graph depicts the mean time course of $I_{Cl(Ca)}$ amplitude elicited by 1 s depolarizing pulses to +90 mV, followed by 1 s repolarizing steps to −80 mV, in the presence of 5 mM ATP ($n = 42$), or with 0 mM ATP + 10 μM KN-93 ($n = 32$). Currents were normalized to the initial current amplitude at the beginning of the protocol. Each step was applied from HP = −50 mV at a frequency of one pulse every 5 s for 10 min. ***Significantly different from cells dialysed with 0 mM ATP and 10 μM KN-93; $P < 0.001$. (B) This graph shows the mean time course of changes of late $I_{Cl(Ca)}$ measured at the end of 1 s steps to +90 mV from HP = −50 mV (one step every 10 s) in cells dialysed with 0 mM ATP, with ($n = 4$) or without ($n = 5$) 10 μM cyclosporine A to inhibit calcineurin. **Significantly different from cells dialysed with 0 mM ATP and 10 μM cyclosporine A; $P < 0.01$.

series of experiments was carried out to further demonstrate that changing ATP levels influenced an important phosphorylation step regulating $I_{Cl(Ca)}$. Figure 1B shows that removing ATP alone also attenuated rundown $I_{Cl(Ca)}$ and led to a recovery of the current that still exceeded the initial level after 10 min but to a lesser extent (~10% instead of 30%) than when KN-93 was included in the pipette solution. As shown in Figure 1B including cyclosporine A in the pipette solution, a specific inhibitor of the Ca^{2+}-dependent phosphatase calcineurin (Klee *et al.*, 1998; Rusnak and Mertz, 2000), prevented the recovery of $I_{Cl(Ca)}$. These experiments established that the very different characteristics of $I_{Cl(Ca)}$ before any exposure to NFA was carried out were dictated by diametrically opposed states of global phosphorylation.

Global state of dephosphorylation enhances the potency of NFA-induced block of $I_{Cl(Ca)}$

The next series of experiments were conducted to determine whether NFA exerts a differential effect on $I_{Cl(Ca)}$ when the state of global phosphorylation is altered. Figure 2A depicts typical experiments in which the effects of 100 μM NFA were tested on $I_{Cl(Ca)}$ recorded from a cell dialysed with 5 mM ATP, and 0 mM ATP and 10 μM KN-93 respectively. The superimposed traces shown to the right of the graph were obtained immediately before (labelled *a*) and after steady-state block achieved by NFA (labelled *b*). The voltage clamp protocol used was similar to that of Figure 1, with changes outlined in the *Methods* section. The graph shows the two superimposed time courses of normalized $I_{Cl(Ca)}$ amplitude before and during the application of NFA. In both cases, NFA blocked the instantaneous and time-dependent components of $I_{Cl(Ca)}$ but the amount of inhibition was notably increased for the cell dialysed with 0 mM ATP and KN-93. Figure 2B shows plots of mean normalized $I_{Cl(Ca)}$ at +90 mV as a function of time for similar experiments performed with a pipette solution containing 5 mM ATP or 0 mM ATP and KN-93. Although the time course of block of $I_{Cl(Ca)}$ by NFA was similar in both groups, the ATP-free pipette solution containing KN-93 clearly enhanced the potency of the drug. On average NFA blocked $I_{Cl(Ca)}$ by 42 ± 10% with 5 mM ATP and 80 ± 3% with no ATP + KN-93. These results demonstrate that inhibition of $I_{Cl(Ca)}$ mediated by a presumed state channel or regulatory subunit phosphorylation reduces the ability of NFA to inhibit the channels.

We next examined the voltage dependence of interaction of NFA under both conditions (Figure 3). On the left hand side of each panel, typical families of $I_{Cl(Ca)}$ currents recorded from the same cell in control (top) and after exposure to 100 μM NFA for 10 min (bottom) are shown. For each panel, the graph on the right hand side reflects the mean I–V relationships of $I_{Cl(Ca)}$ density registered at the end of 1 s steps ranging from −100 to +140 mV from HP = −50 mV and obtained before and after the application of NFA. Consistent with phosphorylation-induced changes in Cl_{Ca} channel gating (Greenwood *et al.*, 2001; 2004; Ledoux *et al.*, 2003; Leblanc *et al.*, 2005; Angermann *et al.*, 2006), control currents recorded with 5 mM ATP (Figure 3A) were considerably smaller (note the different calibration bars), and displayed slower activation and faster deactivation kinetics than those obtained in the absence of ATP (Fig. 3B). For both groups of

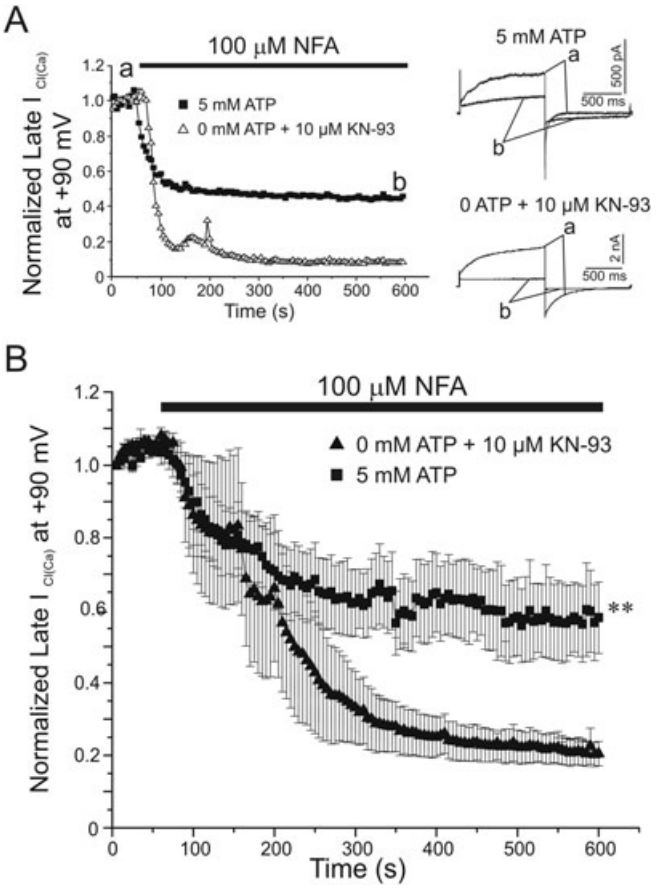

Figure 2 Effect of phosphorylation on the ability of NFA to block $I_{Cl(Ca)}$. (A) Representative time courses from pulmonary artery smooth muscle cells dialysed with pipette solutions containing either 5 mM ATP or 0 mM ATP + 10 μM KN-93. Currents were measured at the end of 1 s depolarizing steps to +90 mV from HP = −50 mV and plotted against time over a 10 min period of dialysis. Following current stabilization, 100 μM NFA was applied to the cells, as indicated by the filled bar. Corresponding to points (a) and (b) on the time courses, superimposed sample traces taken before (a) and after (b) the application of NFA are shown to the right of the graph for each experiment. (B) Time courses representing mean data collected as described above for cells dialysed with 5 mM ATP ($n = 10$) or 0 mM ATP + 10 μM KN-93 pipette solution ($n = 5$). **Significantly different from 5 mM ATP with $P < 0.01$.

cells, NFA blocked instantaneous and time-dependent outward $I_{Cl(Ca)}$ (>0 mV) but the block was greater with 0 mM ATP and KN-93 (Figure 3B) than with 5 mM ATP (Figure 3A). NFA was previously shown to enhance $I_{Cl(Ca)}$ in the negative range of membrane potentials (Piper *et al.*, 2002). The same group also reported marked rebound stimulation of the current in the entire range of membrane potentials examined during washout of the drug and a similar observation was also made for $I_{Cl(Ca)}$ in rabbit coronary myocytes (Ledoux *et al.*, 2005). The insets in the graphs displayed in Figure 3 represent an expanded scale in the negative range of voltages of the I–V relationships of $I_{Cl(Ca)}$ density. The results confirm that NFA stimulated this current at negative potentials without inducing any shifts in reversal potential which matched the equilibrium for Cl^-(~0 mV). While NFA produced stimulation in cells dialysed with 5 mM ATP at potentials negative to –20 mV (Figure 3A), the stimulation was only apparent for potentials negative to –50 mV in cells dialysed with 0 mM ATP and KN-93 (Figure 3B); in fact NFA blocked $I_{Cl(Ca)}$ at potentials between –40 and –10 mV and this led to the appearance of a crossover point at –50 mV (see arrow). Taken together these results suggested that a phosphorylation step might be causing a shift in the voltage dependence of NFA-induced block and stimulation.

To test this hypothesis, the intensity of block or stimulation (as %) by NFA of steady-state $I_{Cl(Ca)}$ was plotted as a function of voltage (Figure 4) and the calculated parameters are presented in Table 1. In Figure 4, the data in 0 mM ATP alone were omitted for the sake of clarity but fell in between those obtained with 5 mM ATP and 0 mM ATP + KN-93 (see Table 1). All data sets could be well fitted by simple Boltzmann relationships. Figure 4 clearly shows that the interaction of NFA with the Cl_{Ca} channel was voltage-dependent and apparently linked to channel gating (see *Discussion*). In the absence of ATP, a significant block of $I_{Cl(Ca)}$ was apparent above –50 mV and saturated around +50 mV. In contrast, steps more positive than +30 mV were required to detect NFA-induced block of $I_{Cl(Ca)}$ with 5 mM ATP. Another interesting feature is the much shallower slope of the relationship obtained with 5 mM versus 0 mM ATP + KN-93 (Figure 4 and Table 1) suggesting a reduced sensitivity to voltage when phosphorylation is promoted. Thus, global phosphorylation has a major impact on the voltage dependence of interaction of the fenamate compound with the channel favouring inhibition over stimulation, both appearing to be functionally linked.

Concentration dependence of NFA interaction with Cl_{Ca} channels altered by phosphorylation

Because of the dual nature of the interaction of NFA with Cl_{Ca} channels (Piper *et al.*, 2002; Ledoux *et al.*, 2005), we postulated that it might be possible to better distinguish the inhibitory and stimulatory effects of NFA on $I_{Cl(Ca)}$ recorded under different states of phosphorylation by examining the effects of a wide range of concentrations (0.1–250 μM) of this compound. Consistent with this possibility, Ledoux *et al.* (2005) showed that NFA blocked and stimulated $I_{Cl(Ca)}$ with different affinities. Figure 5 illustrates the effects of NFA on $I_{Cl(Ca)}$ elicited by the standard step protocol described in Figure 1 and depicted at the bottom. Each trace is an average of five traces from four to eight cells recorded immediately prior to, or after a steady-state effect of NFA was observed after 10 min. Interestingly 0.1 mM NFA consistently stimulated the outward current at +80 mV and tail current at –80 mV as well as the steady-state current at the HP in cells dialysed with 5 mM ATP (upper left traces). In contrast, in cells dialysed with 0 mM ATP and KN-93, the same concentration of NFA produced inhibition of the outward current at +80 mV, a slight inhibition of the peak inward tail current at –80 mV, and stimulation of steady-state current as evident from the tail current deactivating to a higher negative level (upper right traces). Increasing the concentration of NFA to 10 μM converted the stimulation to block at +80 mV with 5 mM ATP (middle left traces), little effect on peak inward tail current at –80 mV but a profound and well-characterized slowing of deactivation (Hogg *et al.*, 1994; Greenwood and Large, 1996). In the absence of substrate, NFA produced a more potent inhibition

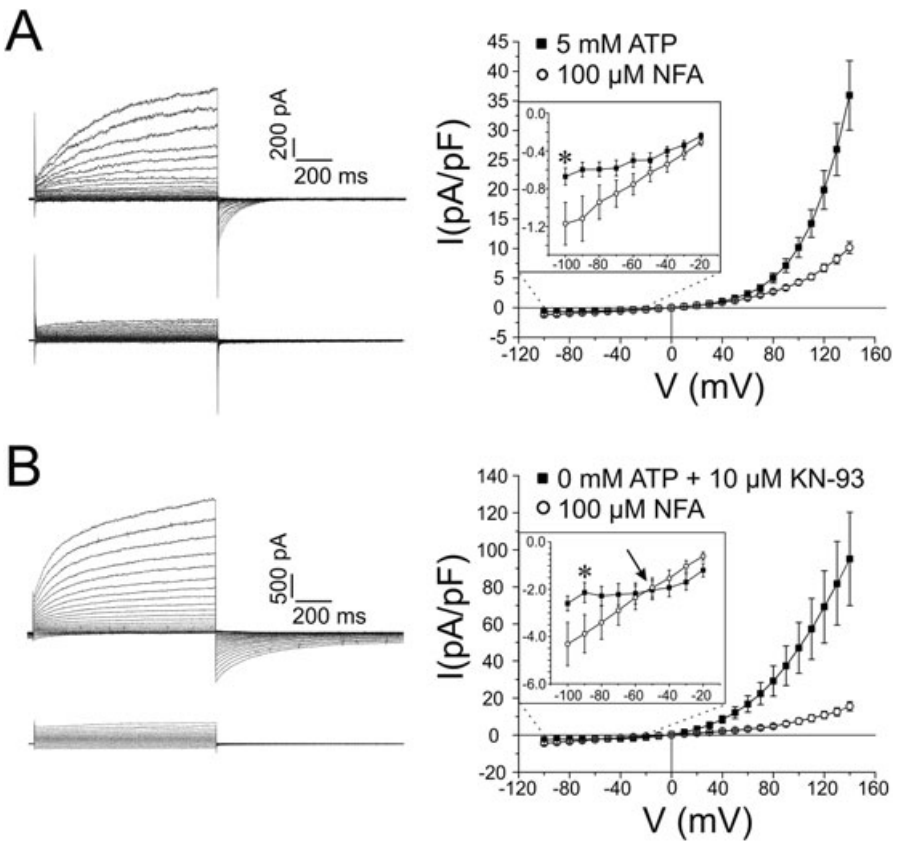

Figure 3 The voltage dependence of $I_{Cl(Ca)}$ block by NFA is altered by phosphorylation levels. (A) On the left, two representative families of currents from a cell dialysed with 5 mM ATP, before (upper) and after (lower) a 10 min application of 100 μM NFA. Currents were evoked by stepping in 10 mV increments from HP = –50 mV to 1 s test potentials ranging from –100 mV to +140 mV following a 10 min period of dialysis. On the right, mean current–voltage relationships generated from similar families of currents after 10 min of cell dialysis with 5 mM ATP (n = 10), and after 10 min with the addition of 100 μM NFA to the external solution (n = 10). The inset highlights an expanded segment of the current–voltage relationship from –100 mV to –20 mV. (B) was generated in a similar fashion to (A) except for the fact that in (B), cells were dialysed with a pipette solution containing 0 mM ATP + 10 μM KN-93 (n = 5). Please note in (B) the negative shift in voltage where block is converted to stimulation when phosphorylation is minimized (indicated by the arrow in the inset). $^*P < 0.05$.

of the time-dependent outward current at +80 mV and tail current at –80 mV; as with ATP, NFA markedly slowed deactivation kinetics of $I_{Cl(Ca)}$ which crossed over with the control current (middle right traces). Increasing NFA concentration to 250 μM led to more potent block of the current at +80 mV, and now a significant but small inhibition of the peak inward tail current at –80 mV accompanied by the typical slowing of deactivation kinetics at –80 mV with a detectable cross-over with the control current (lower left traces). With 0 mM ATP and KN-93, the same concentration of NFA led to marked block of the outward and inward $I_{Cl(Ca)}$ at +80 and –80 mV respectively; it is apparent that the cross-over described above disappeared because of the marked inhibition of the inward tail current.

Figure 6 reports mean data for all NFA concentrations tested on $I_{Cl(Ca)}$ measured at the end of the step to +80 mV (Figure 6A) and peak inward tail current at –80 mV (Figure 6B). For both graphs, % block or % stimulation is indicated by a negative or positive value respectively. With 0 mM ATP and KN-93, NFA dose-dependently blocked the outward and inward current relaxations with an IC_{50} of ~ 46 μM. We were also unable to observe stimulation of $I_{Cl(Ca)}$ when testing even lower concentrations of NFA (0.1 μM, n = 3; 1 μM, n = 4; and 10 μM, n = 3). Enabling global phosphorylation with 5 mM ATP led to a significant stimulation of the outward current at +80 mV with 0.1 μM NFA, and inward tail current at –80 mV in the range of 0.1–10 μM NFA. 100 and 250 μM NFA led to significant inhibition of both current components but the magnitude of block was considerably reduced relative to cells dialysed with 0 mM ATP and KN-93. Taken together, these results provide convincing evidence for a direct impact of the presumed state of phosphorylation on the ability of NFA to inhibit and stimulate Cl_{Ca} channels.

Discussion

This study reports for the first time, the effect of a presumed state of phosphorylation in the channel or regulatory subunit, on the interaction of NFA on native Ca^{2+}-activated Cl^- currents recorded in freshly isolated rabbit pulmonary arterial smooth muscle cells. $I_{Cl(Ca)}$ elicited by sustained elevated intracellular Ca^{2+} concentration under conditions favouring either phosphorylation or dephosphorylation led to very marked differences in sensitivity to NFA. NFA produces a paradoxical dual effect on $I_{Cl(Ca)}$ in pulmonary artery

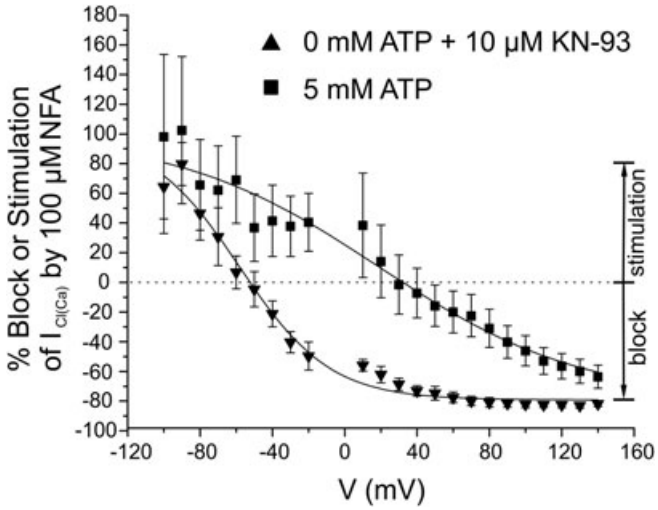

Figure 4 Altering global phosphorylation status shifts the voltage dependence of the dual effect of NFA on $I_{Cl(Ca)}$. The two data sets were obtained after 10 min of cell dialysis with either 5 mM ATP or 0 mM ATP + 10 μM KN-93 pipette solutions, before and after addition of 100 μM NFA. % Block was determined at each individual voltage step for each cell using the formula $((I_{NFA}/I_{Control})*100) - 100$, where I_{NFA} and $I_{Control}$ is the current recorded in the presence and absence of NFA respectively. For $I_{Control}$, the mean of the first five traces was used in the calculation, while for I_{NFA} the mean of the last five stable traces was used. Stimulation appears as a positive value using the above formula and is shown as such. Mean values were then plotted at each voltage, and fitted to a Boltzmann function. Parameters estimated from these fits are presented in Table 1.

myocytes, stimulating and blocking the channels at negative and positive potentials respectively (Piper *et al.*, 2002). Analysis of the voltage dependence of interaction of NFA with $I_{Cl(Ca)}$ showed that although the maximal level of block at positive potentials and stimulation at negative potentials were similar, promoting global dephosphorylation shifted the voltage at which block was 'apparently' converted to stimulation by more than –70 mV. Examination of the concentration dependence of the interaction revealed that a very low concentration of NFA (100 nM) led to stimulation of fully activated $I_{Cl(Ca)}$ at +80 mV and tail current at –80 mV in cells dialysed with ATP to support global phosphorylation; stimulation was converted to block between 1 and 10 μM NFA and higher concentrations inhibited the current, albeit to a lower extent than for cells dialysed with 0 mM ATP and 10 μM KN-93. In contrast, $I_{Cl(Ca)}$ in cells dialysed with 0 mM ATP and KN-93 was blocked in a concentration-dependent manner by NFA in the range of 0.1–250 μM. These results demonstrate that alteration of Cl_{Ca} channel gating by an unidentified phosphorylation step profoundly influences the mode of interaction of NFA with the channel.

Conditions establishing global states of phosphorylation

Ca^{2+}-activated Cl^- channels in airway and arterial myocytes are subject to Ca^{2+}-dependent suppression when intracellular Ca^{2+} levels are raised and this process involves activation of Ca^{2+}-calmodulin and CaMKII (Wang and Kotlikoff, 1997; Greenwood *et al.*, 2001). Phosphorylation by CaMKII of an unknown target on the channel protein or closely associated accessory regulator protein results in a time-dependent decline of $I_{Cl(Ca)}$ that is faster than the Ca^{2+} transient triggering channel opening (Wang and Kotlikoff, 1997), or current rundown when intracellular Ca^{2+} levels are clamped above 200 nM (Angermann *et al.*, 2006). It is hypothesized that CaMKII-induced inhibition of $I_{Cl(Ca)}$ serves an important role in attenuating the strong depolarizing influence of Cl_{Ca} channels during excitation (Leblanc *et al.*, 2005). This 'braking' or negative feedback regulation by CaMKII is antagonized by calcineurin in rabbit coronary (Ledoux *et al.*, 2003) and pulmonary artery (Greenwood *et al.*, 2004). Several of our present findings – the extensive rundown of $I_{Cl(Ca)}$ seen in our study when phosphorylation is supported by 5 mM ATP in the pipette solution, the substantial recovery of the current in myocytes supplied internally with 0 mM ATP with or without KN-93, and the inhibition of the delayed recovery by the calcineurin inhibitor cyclosporine A – are consistent with this hypothesis. These findings are compatible with recent work from our group contrasting the effects of cell dialysis with 3 mM ATP or 3 mM AMP-PNP, a non-hydrolysable analogue of ATP (Angermann *et al.*, 2006). Also in accord with this idea, the higher ATP concentration used in the present study (5 vs. 3 mM in Angermann *et al.*, 2006) enhanced the rate and magnitude of $I_{Cl(Ca)}$ rundown. Angermann *et al.* (2006) proposed a kinetic model whereby phosphorylation induces state-dependent block through voltage-dependent gating steps favouring closure at high levels of Ca^{2+} occupancy on the cytoplasmic side of the channel. This model predicts more rapid activation at positive potentials and slower deactivation kinetics at negative potentials at high $[Ca^{2+}]_i$ when the channel or an unknown regulatory element is dephosphorylated by endogenous phosphatases. Currents elicited in cells supplied with 0 mM ATP and KN-93 to inhibit CaMKII, activated more quickly and deactivated more slowly than those dialysed with 5 mM ATP. Our results thus firmly establish that the underlying pore-forming or regulatory subunit of Cl_{Ca} channels was either extensively phosphorylated (5 mM ATP) or dephosphorylated (0 mM ATP, with or without KN-93) after 10 min of cell dialysis, prior to any application of drug.

Global phosphorylation attenuates the block of $I_{Cl(Ca)}$ by NFA

Our first series of experiments were designed to examine the effects of 100 μM NFA, a widely used concentration, on presumed phosphorylated and dephosphorylated Cl_{Ca} channels. The rationale for these experiments was based on the observation that NFA preferentially interacts with open Cl_{Ca} channels and that the block is voltage-dependent (Hogg *et al.*, 1994; Large and Wang, 1996). We thus hypothesized that presumed phosphorylation-induced channel closure might reduce the ability of NFA to block $I_{Cl(Ca)}$. Our data confirmed this hypothesis by showing that steady-state block at +90 mV by this compound was significantly greater in cells lacking ATP. Although the maximal levels of achievable inhibition or stimulation were similar, analysis of the voltage dependence of the interaction of NFA with the channels revealed striking differences. For presumed dephosphorylated channels, the block was sharply voltage-dependent below 0 mV and stimulation was apparent below –50 mV. In contrast, stimulation was evident at potentials negative to +20 mV in cells dialysed

Table 1 Voltage-dependent parameters describing the interaction of niflumic acid with Ca^{2+}-activated Cl^- currents ($I_{Cl(Ca)}$) recorded from pulmonary artery myocytes

	$V_{0.5}$ (mV)	*Slope (mV)*	*V where y = 0 (mV)*
5 mM ATP	+16.0 ± 2.1	59.2 ± 3.9	29.7
0 ATP	–8.9 ± 3.5	24.2 ± 3.1	–3.3
0 ATP + 10 μM KN-93	–59.7 ± 0.8	26.1 ± 1.5	–53.7

Half-maximal voltage ($V_{0.5}$) and slope values were estimated by curve fitting of the data plotted in Figure 4 (except for the data with 0 mM ATP alone which was not shown) to a Boltzmann equation. V where $y = 0$ represents the voltage where the fitted Boltzmann relationships cross the *y*-axis and corresponds to the voltage at which conversion from block to stimulation by niflumic acid was observed.

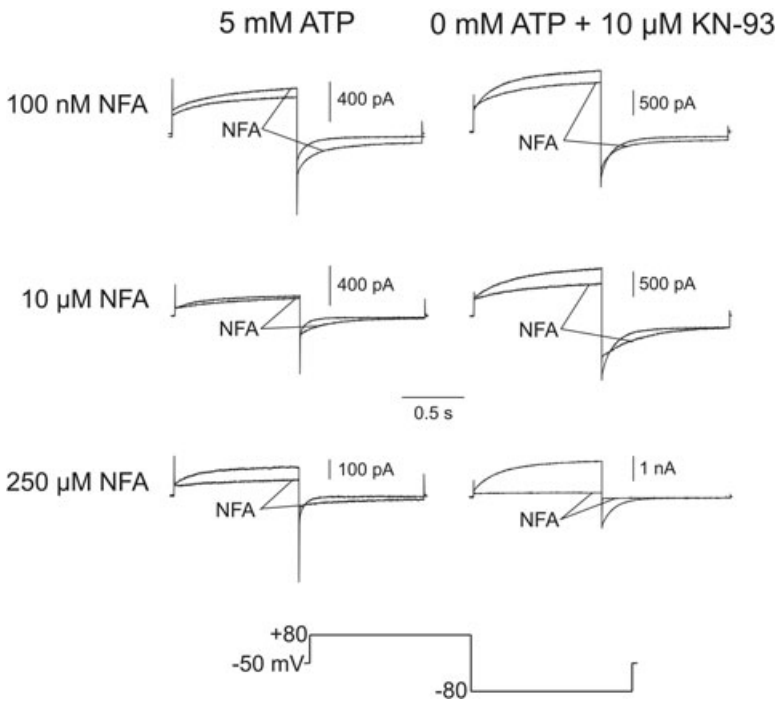

Figure 5 Effects of various concentrations of NFA on representative $I_{Cl(Ca)}$ traces recorded from cells under different states of global phosphorylation. Average currents are shown before and after application of NFA in cells dialysed with 5 mM ATP, or 0 mM ATP + 10 μM KN-93. Current were elicited by 1 s repetitive depolarizing steps from HP = –50 mV to +80 mV, each followed by a 1 s repolarizing step to –80 mV to record tail current. Averaged traces were calculated using Clampfit 9.2 (Molecular Devices). For unmarked control currents, the first five stable traces at the end of 10 min of cell dialysis were averaged for each cell, and subsequently averaged to give a mean current trace for the entire group of cells. Following a 10 min application of NFA, currents (marked 'NFA') were similarly averaged. Note the concentration-dependent effect of NFA on deactivation kinetics by comparing the effect of 10 μM NFA on $I_{Cl(Ca)}$ in cells dialysed with 5 mM ATP ($n = 6$), or 0 mM ATP + 10 μM KN-93 ($n = 3$), to the effect of 250 μM NFA on cells dialysed with 5 mM ATP ($n = 3$), or 0 mM ATP + 10 μM KN-93 ($n = 3$).

with 5 mM ATP whereas block was only apparent at potentials more positive than +20 mV. These data suggest that presumed phosphorylation reduces the blocking efficacy of NFA, an effect that may favour the unmasking of the stimulatory effect of NFA. Whether these two opposing effects of NFA are independent as previously suggested by our group for the effects of NFA on $I_{Cl(Ca)}$ in rabbit coronary artery myocytes (Ledoux *et al.*, 2003) will require more investigation. One possibility to explain these observations is that the NFA binding site responsible for blocking the channel becomes more easily accessible by channel opening, a situation favoured by presumed dephosphorylation; consistent with this idea was the observation that cell dialysis with 500 nM Ca^{2+} and 3 mM AMP-PNP caused an elevation of basal Cl_{Ca} channel conductance between –100 and –50 mV, and increased progressively from –50 to +130 mV (Angermann *et al.*, 2006). This contrasted with Cl_{Ca} conductance in myocytes dialysed with 5 mM ATP which was very small from –100 to ~0 mV and increased sharply beyond this voltage. An alternative explanation is that presumed phosphorylation favoured NFA-mediated stimulation that counteracted inhibition.

Pharmacological significance

To our knowledge, there is only one other study demonstrating the impact of altered channel gating because of phosphorylation on the pharmacology of an anion channel. Derand *et al.* (2003) showed that the activation of the cystic fibrosis transmembrane conductance regulator (CFTR) anion channel by a benzimidazolone, NS004, was influenced by the state of

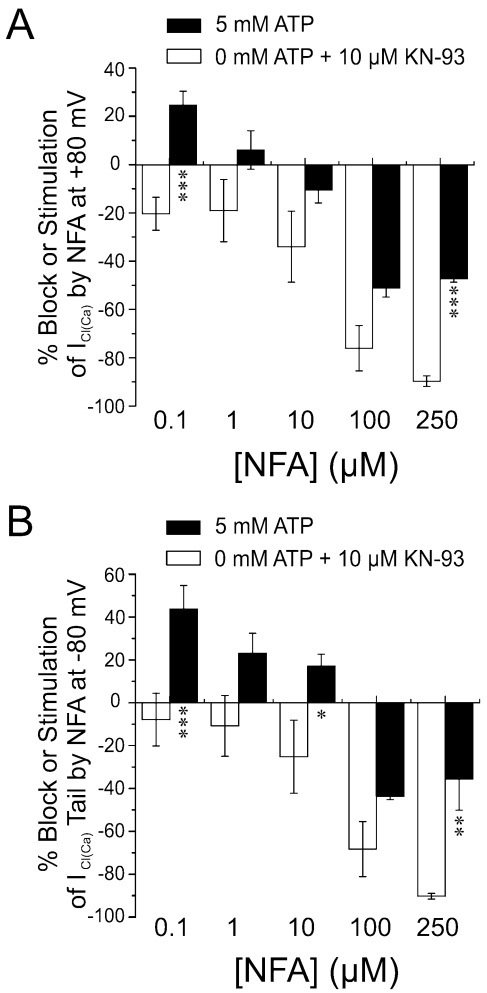

Figure 6 Concentration dependence of the dual effect of NFA on $I_{Cl(Ca)}$. (A) In cells dialysed with either 5 mM ATP (filled bars), or 0 mM ATP + 10 μM KN-93, NFA was added for 10 min at concentrations of 0.1, 1, 10, 100 and 250 μM. Current was recorded at the end of 1 s depolarizing pulses to +80 mV from HP of −50 mV, and % block for each cell was calculated by the formula $((I_{NFA}/I_{Control})*100) - 100$, where I_{NFA} and $I_{Control}$ are the currents recorded in the presence and absence of NFA respectively. For $I_{Control}$, the mean of the first five traces was used in the calculation, while for I_{NFA} the mean of the last five stable traces was used. Stimulation appears as a positive value using the above formula, and is shown as such. Mean calculated values were then determined for each group (5 mM ATP: 0.1 μM NFA, $n = 8$; 1 μM NFA, $n = 5$, 10 μM NFA, $n = 6$; 100 μM NFA, $n = 4$; 250 μM NFA, $n = 4$; 0 mM ATP + 10 μM KN-93: 0.1 μM NFA, $n = 7$; 1 μM NFA, $n = 4$; 10 μM NFA, $n = 3$; 100 μM NFA, $n = 5$; 250 μM NFA, $n = 4$) and graphed. Panel (B) was generated similarly to (A), but the instantaneous tail current was recorded upon repolarizing the cell to −80 mV for 1 s following the depolarizing step described in (A). Note that while low concentrations of NFA stimulated $I_{Cl(Ca)}$ at +80 mV and −80 mV when cells were dialysed with 5 mM ATP, in cells dialysed with 0 mM ATP + 10 μM KN-93 only block by NFA was detected. $^{*}P < 0.05$; $^{**}P < 0.01$; $^{***}P < 0.001$ (unpaired Student's *t*-tests).

phosphorylation of the R domain by cAMP-dependent protein kinase. This compound was shown to activate phosphorylated CFTR with an EC_{50} of 11 μM while an EC_{50} in excess of 100 μM was determined for non-phosphorylated CFTR channels. Derand *et al.* (2003) suggested that phosphorylation facilitates binding site accessibility through domain interactions or conformational changes. We propose a similar paradigm, albeit in the opposite direction, for the attenuated ability of NFA to inhibit presumed phosphorylated Cl_{Ca} channels. CaMKII-induced phosphorylation may occlude the binding site by voltage-dependent steric hindrance, or by reduced availability through a state-dependent mechanism.

The present study offers some interesting clues relating to the relatively wide range of IC_{50} values for NFA to block $I_{Cl(Ca)}$ in VSMCs. In the first comprehensive description of the mechanism of block of this current in rabbit portal vein smooth muscle cells, Hogg *et al.* (1994) showed that NFA blocked STICs produced by Cl_{Ca} channels with an IC_{50} of ~1–4 μM. 10 μM NFA blocked the slow inward $I_{Cl(Ca)}$ tail evoked by Ca^{2+} entry through L-type Ca^{2+} channels (I_{CaL}) by 71% in rabbit coronary artery (Lamb *et al.*, 1994), implying an EC_{50} value below that concentration. In the same preparation, NFA reduced $I_{Cl(Ca)}$ elicited by sustained 500 nM Ca^{2+} with a much higher IC_{50} (159 μM; Ledoux *et al.*, 2005). One important difference in the methods used to elicit $I_{Cl(Ca)}$ is that STICs and I_{CaL}-induced $I_{Cl(Ca)}$ are evoked by transient elevations of $[Ca^{2+}]_i$. Autophosphorylation of CaMKII may be quite limited; in fact, the phosphorylation balance is likely to be shifted towards a dephosphorylation state as calcineurin displays about two orders of magnitude higher affinity for Ca^{2+}-CaM than CaMKII and is directly activated by Ca^{2+} via an interaction with the B subunit of calcineurin (Abraham *et al.*, 1996; Klee *et al.*, 1998; Rusnak and Mertz, 2000; Ledoux *et al.*, 2003). These results suggest caution when using NFA as a pharmacological tool to assess the role of Cl_{Ca} channels in controlling vascular tone. Large sustained elevations in $[Ca^{2+}]_i$ caused by high concentrations of constricting agonists is likely to promote a higher state of phosphorylation of Cl_{Ca} channels and reduced efficacy of NFA. Indeed, a study by Remillard *et al.* (2000) showed a progressive attenuation of NFA-induced vasorelaxation of pressurized rabbit mesenteric small arteries when the concentration of the α_1-adrenoceptor agonist, phenylephrine, was raised from 100 nM to 10 μM. The recent discoveries of the Bestrophin (Leblanc *et al.*, 2005; Hartzell *et al.*, 2008) and TMEM16A/B genes (Caputo *et al.*, 2008; Schroeder *et al.*, 2008; Yang *et al.*, 2008) as novel molecular candidates for Cl_{Ca} genes will soon bring novel insight into the mechanisms regulating their activation by Ca^{2+}, voltage and phosphorylation, and how the interplay of these factors influences their pharmacology.

Acknowledgements

We thank Catherine Lachendro, Janice Tinney and Marissa Huebner for their technical support in isolating pulmonary artery smooth muscle cells and preparing solutions. This study was supported by a grant to NL from the National Institutes of Health (Grant 5 RO1 HL 075477) and a grant to IAG from the British Heart Foundation (PG/ 05/ 038). The publication was also made possible by a grant to NL (NCRR 5 P20 RR15581) from the National Center for Research Resources, a component of the National Institutes of Health (NIH) supporting two Centers of Biomedical Research Excellence (COBRE) at the University of Nevada School of Medicine, Reno, Nevada. The contents of the manuscript are solely

the responsibility of the authors and do not necessarily represent the official views of NCRR or NIH.

Conflicts of interest

None.

References

Abraham ST, Benscoter H, Schworer CM, Singer HA (1996). In situ Ca^{2+} dependence for activation of Ca^{2+}/calmodulin-dependent protein kinase II in vascular smooth muscle cells. *J Biol Chem* **271**: 2506–2513.

Angermann JE, Sanguinetti AR, Kenyon JL, Leblanc N, Greenwood IA (2006). Mechanism of the inhibition of Ca^{2+}-activated Cl- currents by phosphorylation in pulmonary arterial smooth muscle cells. *J Gen Physiol* **128**: 73–87.

Caputo A, Caci E, Ferrera L, Pedemonte N, Barsanti C, Sondo E et al. (2008). TMEM16A, a membrane protein associated with calcium-dependent chloride channel activity. *Science* **322**: 590–594.

Clapp LH, Turner JL, Kozlowski RZ (1996). Ca^{2+}-activated Cl- currents in pulmonary arterial myocytes. *Am J Physiol Heart Circ Physiol* **39**: H1577–H1584.

Criddle DN, de Moura RS, Greenwood IA, Large WA (1996). Effect of niflumic acid on noradrenaline-induced contractions of the rat aorta. *Br J Pharmacol* **118**: 1065–1071.

Criddle DN, de Moura RS, Greenwood IA, Large WA (1997). Inhibitory action of niflumic acid on noradrenaline- and 5-hydroxytryptamine-induced pressor responses in the isolated mesenteric vascular bed of the rat. *Br J Pharmacol* **120**: 813–818.

Derand R, Bulteau-Pignoux L, Becq F (2003). Comparative pharmacology of the activity of wild-type and G551D mutated CFTR chloride channel: effect of the benzimidazolone derivative NS004. *J Membr Biol* **194**: 109–117.

Greenwood IA, Large WA (1995). Comparison of the effects of fenamates on Ca-activated chloride and potassium currents in rabbit portal vein smooth muscle cells. *Br J Pharmacol* **116**: 2939–2948.

Greenwood IA, Large WA (1996). Analysis of the time course of calcium-activated chloride 'tail' currents in rabbit portal vein smooth muscle cells. *Pflugers Arch* **432**: 970–979.

Greenwood IA, Large WA (1998). Properties of a Cl^- current activated by cell swelling in rabbit portal vein vascular smooth muscle cells. *Am J Physiol Heart Circ Physiol* **275**: H1524–H1532.

Greenwood IA, Ledoux J, Leblanc N (2001). Differential regulation of Ca^{2+}-activated Cl^- currents in rabbit arterial and portal vein smooth muscle cells by Ca^{2+}-calmodulin-dependent kinase. *J Physiol* **534**: 395–408.

Greenwood IA, Ledoux J, Sanguinetti A, Perrino BA, Leblanc N (2004). Calcineurin Aα but not Aβ augments $I_{Cl(Ca)}$ in rabbit pulmonary artery smooth muscle cells. *J Biol Chem* **279**: 38830–38837.

Hartzell HC, Qu Z, Yu K, Xiao Q, Chien LT (2008). Molecular physiology of bestrophins: multifunctional membrane proteins linked to best disease and other retinopathies. *Physiol Rev* **88**: 639–672.

Hogg RC, Wang Q, Large WA (1994). Action of niflumic acid on evoked and spontaneous calcium-activated chloride and potassium currents in smooth muscle cells from rabbit portal vein. *Br J Pharmacol* **112**: 977–984.

Janssen J, Sims SM (1994). Spontaneous transient inward currents and rhythmicity in canine and guinea-pig tracheal smooth muscle cells. *Pflugers Arch* **427**: 473–480.

Klee CB, Ren H, Wang XT (1998). Regulation of the calmodulin-stimulated protein phosphatase, calcineurin. *J Biol Chem* **273**: 13367–13370.

Lamb FS, Barna TJ (1998). Chloride ion currents contribute functionally to norepinephrine-induced vascular contraction. *Am J Physiol Heart Circ Physiol* **275**: H151–H160.

Lamb FS, Volk KA, Shibata EF (1994). Calcium-activated chloride current in rabbit coronary artery myocytes. *Circ Res* **75**: 742–750.

Large WA, Wang Q (1996). Characteristics and physiological role of the Ca^{2+}-activated Cl^- conductance in smooth muscle. *Am J Physiol Cell Physiol* **271**: C435–C454.

Leblanc N, Leung PM (1995). Indirect stimulation of Ca^{2+}-activated Cl^- current by Na^+/Ca^{2+} exchange in rabbit portal vein smooth muscle. *Am J Physiol Heart Circ Physiol* **268**: H1906–H1917.

Leblanc N, Ledoux J, Saleh S, Sanguinetti A, Angermann J, O'Driscoll K et al. (2005). Regulation of calcium-activated chloride channels in smooth muscle cells: a complex picture is emerging. *Can J Physiol Pharmacol* **83**: 541–556.

Ledoux J, Greenwood I, Villeneuve LR, Leblanc N (2003). Modulation of Ca^{2+}-dependent Cl^- channels by calcineurin in rabbit coronary arterial myocytes. *J Physiol* **552**: 701–714.

Ledoux J, Greenwood IA, Leblanc N (2005). Dynamics of Ca^{2+}-dependent Cl^- channel modulation by niflumic acid in rabbit coronary arterial myocytes. *Mol Pharmacol* **67**: 163–173.

Pacaud P, Loirand G, Lavie JL, Mironneau C, Mironneau J (1989). Calcium-activated chloride current in rat vascular smooth muscle cells in short-term primary culture. *Pflugers Arch* **413**: 629–636.

Piper AS, Greenwood IA, Large WA (2002). Dual effect of blocking agents on Ca^{2+}-activated Cl^- currents in rabbit pulmonary artery smooth muscle cells. *J Physiol* **539**: 119–131.

Remillard CV, Lupien MA, Crepeau V, Leblanc N (2000). Role of Ca^{2+}- and swelling-activated Cl^- channels in a_1-adrenoceptor-mediated tone in pressurized rabbit mesenteric arterioles. *Cardiovasc Res* **46**: 557–568.

Rusnak F, Mertz P (2000). Calcineurin: Form and function. *Physiol Rev* **80**: 1483–1521.

Schroeder BC, Cheng T, Jan YN, Jan LY (2008). Expression cloning of TMEM16A as a calcium-activated chloride channel subunit. *Cell* **134**: 1019–1029.

Wang YX, Kotlikoff MI (1997). Inactivation of calcium-activated chloride channels in smooth muscle by calcium/calmodulin-dependent protein kinase. *Proc Natl Acad Sci USA* **94**: 14918–14923.

Yang YD, Cho H, Koo JY, Tak MH, Cho Y, Shim WS et al. (2008). TMEM16A confers receptor-activated calcium-dependent chloride conductance. *Nature* **455**: 1210–1215.

Yuan XJ (1997). Role of calcium-activated chloride current in regulating pulmonary vasomotor tone. *Am J Physiol Lung Respir Physiol* **272**: L959–L968.

ZhuGe RH, Sims SM, Tuft RA, Fogarty KE, Walsh JV (1998). Ca^{2+} sparks activate K^+ and Cl^- channels, resulting in spontaneous transient currents in guinea-pig tracheal myocytes. *J Physiol* **513**: 711–718.